Simulation of Electron Transfer between Cytochrome c_2 and the Bacterial Photosynthetic Reaction Center: Brownian Dynamics Analysis of the Native Proteins and Double Mutants

Jianping Lin and David N. Beratan*

Departments of Chemistry and Biochemistry, Duke University, Durham, North Carolina 27708

Received: October 7, 2004; In Final Form: January 22, 2005

Electron transfer is essential for bacterial photosynthesis which converts light energy into chemical energy. This paper theoretically studies the interprotein electron transfer from cytochrome c_2 of *Rhodobacter capsulatus* to the photosynthetic reaction center of *Rhodobacter sphaeroides* in native and mutated systems. Brownian dynamics is used with an exponential distance-dependent electron-transfer rate model to compute bimolecular rate constants, which are consistent with experimental data when reasonable prefactors and decay constants are used. Interestingly, switching of the reaction mechanism from the diffusion-controlled limit in the native proteins to the activation-controlled limit in one of the mutants (DK(L261)/KE(C99)) was found. We also predict that the second-order rate for the native reaction center/cytochrome c_2 system will decrease with increasing ionic strength, a characteristic of electrostatically controlled docking.

1. Introduction

In bacterial photosynthesis, electron transfer to the reaction center special pair[1] from a cytochrome[2] completes the cycle of converting light energy into chemical energy. Electron transfer to the reaction center in *Rhodobacter sphaeroides* occurs from cytochrome c_2. This cytochrome binds reversibly to the reaction center; the reaction is intermolecular. Experimentally, the kinetics involved in the association and electron transfer between cytochrome c_2 and the reaction center has been studied extensively.[3−8] The following reaction scheme summarizes the binding, excitation, and electron-transfer events (cyt = cytochrome c_2; DQ = reaction center).[8]

$$\begin{array}{ccc} \mathrm{cyt}^{2+} + \mathrm{DQ} & \overset{K_A = 1/K_D}{\rightleftharpoons} & \mathrm{cyt}^{2+}{:}\mathrm{DQ} \\ h\nu \downarrow & & h\nu \downarrow \\ \mathrm{cyt}^{2+} + \mathrm{D}^{+}\mathrm{Q}^{-} & \overset{k_2}{\rightleftharpoons} & \mathrm{cyt}^{2+}{:}\mathrm{D}^{+}\mathrm{Q}^{-} \xrightarrow{k_e} \mathrm{cyt}^{3+}{:}\mathrm{DQ}^{-} \end{array}$$

Following photooxidation and electron transfer, the reaction center is in the D^+Q^- state. The electron-transfer kinetics between the native reaction center and cytochrome c_2 displays two phases in the experiments, a first-order phase with a rate constant k_e of 1.1×10^6 s^{-1}, presumably arising from the cytochrome c_2-bound reaction center species, and a second-order phase, $k_2 \approx 1.6 \times 10^9$ s^{-1} M^{-1} (at pH 7.5, 10 mM ionic strength)[8] that apparently arises from diffusion-limited electron transfer (see the Appendix for a definition of these limits). Several groups[7−10] have studied the influence of protein mutations on the reaction center-cytochrome c_2 electron-transfer kinetics by manipulating the charge-complementary residues on the surfaces of the two proteins (Tyrosine 162 of the reaction center L-subunit, for example).

Because of the wide range of docking geometries accessible in the interprotein electron transfer, these processes have received relatively limited theoretical attention compared to unimolecular electron transfer. For systems with electron-transfer rates close to the diffusion regime, Wade[11−13] and Northrup[14,15] explored the kinetics using Brownian dynamics simulation and obtained second-order electron-transfer rate constants that were comparable with the experimental values. Northrup[16−18] also developed a Brownian dynamics method that spans the diffusion and activation regimes. Kidd and co-workers[19] studied the formation of docked complexes and electron transfer between reduced cytochrome b_5 and oxidized hemoglobin using Brownian dynamics simulations. Recently, Hoffman and co-workers[20] developed a Monte Carlo functional-docking method that describes the interprotein electron transfer in the activation-limited regime. Few detailed simulations on interprotein photosynthetic electron transfer have been carried out because of the size of the proteins involved. Initial exploratory studies of Onuchic and co-workers[21,22] probed the effects of protein dynamics and docking on electron transfer in *Rhodobacter sphaeroides*. Recently, Onuchic, Okamura, and co-workers[23−25] examined the question of how the electron transfer in *Rhodobacter sphaeroides* is influenced by the protein environment and electrostatic interactions between the proteins. Luthey-Schulten and co-workers very recently simulated the protein−protein interface.[26]

In this paper, we use the Brownian dynamics approach of Northrup and co-workers[16−18] to compute the bimolecular interprotein electron-transfer rates between the *Rhodobacter sphaeroides* photosynthetic reaction center and *Rhodobacter capsulatus* cytochrome c_2.[8] We also perform calculations on double mutants (one mutation to the reaction center protein and one mutation to the cytochrome c_2 protein) to explore the influence of electrostatic interactions on the electron-transfer event, and we compare these results with the experimental data.[8] These studies probe the hypothesis that specific *electrostatic steering*[27,28] facilitates the photosynthetic reaction center/cytochrome c_2 electron transfer. We find that change mutations to this electron-transfer pair may cause a mechanistic change in the bimolecular rate from the diffusion-limited regime to the activation-limited regime.

2. Theoretical Method

We utilized the Ermark−McCammon algorithm[29] to solve the diffusion equation for cytochrome c_2 in the electrostatic field

10.1021/jp045417w CCC: $30.25
Published on Web 03/26/2005

of the reaction center. The translational displacement of the relative separation vector **r** in a time step Δt is[12]

$$\Delta \mathbf{r} = \frac{D\Delta t}{k_B T}\mathbf{F} + \mathbf{S} \tag{1}$$

where **F** is the interprotein force, T is the temperature, D is the diffusion constant, k_B is Boltzmann's constant, and S_j (a component of vector **S**) is a random displacement described by a Gaussian distribution with zero mean and $\langle S_j^2 \rangle = 2D\Delta t$ with $j = 1, 2, 3$. Similarly, the rotation angle $\mathbf{w}_i$ of the protein is given by[12]

$$\Delta \mathbf{w}_i = \frac{D_{iR}\Delta t}{k_B T}\mathbf{T}_{ij} + \mathbf{W}_i \tag{2}$$

where D_{iR} is the rotational diffusion constant for each protein, $\mathbf{T}_{ij}$ is the torque acting on protein i because of protein j, and $\boldsymbol{W}_i$ is a random angle described by a Gaussian distribution with $\langle \mathbf{W}_i \rangle = 0$, $\langle W_{ik}^2 \rangle = 2D_{iR}\Delta t$, and $k = 1, 2, 3$.

To calculate the second-order bimolecular rate, we begin the Brownian simulation at a sufficiently large center-to-center separation distance b[30] (where $r > b$ and the interaction force is centrosymmetric). We end the simulation when the two proteins reach a separation, c. The rate constant k is given by[30]

$$k = \frac{k(b)\cdot\beta'}{1 - (1 - \beta')\cdot k(b)/k(c)} \tag{3}$$

where $k(x)$ is the rate constant for diffusion to a relative separation x. In the case of no interaction forces at separations greater than or equal to distance b, $k(x)$ is given by the Smoluchowski expression for the diffusion of two spheres,[31] $k(x) = 4\pi Dx$, where D is the translational diffusional constant for relative motion. β' is the survival probability that satisfies the reaction criterion. We will use the reaction criterion described below to calculate β'.

Northrup[16−18] developed a Brownian dynamics method with an exponential distance-dependent electron-transfer reaction rate criterion that describes the dynamics from the diffusion to the activation limit. The distance-dependent electron-transfer rate constant $k_{et}(d)$ is approximated by

$$k_{et}(d) = k_{et}^0 \exp[-\beta(d - d_0)] \tag{4}$$

where k_{et}^0 is the rate constant when the two proteins are docked with a distance d_0 between donor and acceptor cofactors. β is the distance decay factor.

In the Brownian dynamics model, the intrinsic rate constant $k_{et}(d)$ is dynamically coupled to the diffusional dynamics. For each Brownian step Δt, the probability that the reactant−protein pair survives without electron transfer is

$$p(d) = \exp[-k_{et}(d)\Delta t] \tag{5}$$

and the survival probability is multiplicative throughout the trajectory. As such, the reaction probability for a trajectory is

$$w = 1 - \prod_{i=1}^{j} p_i(d) \tag{6}$$

Here, i is the time step and j is the number of total time steps in the trajectory. As such

$$\beta' = \sum_{l=1}^{N} w_l/N \tag{7}$$

where l is the trajectory number and N is the total number of trajectories.

3. Protein Structural Models and Parameters

Structure. The crystal structures of the reaction center (from *Rhodobacter sphaeroides*) and cytochrome c_2 (from *Rhodobacter capsulatus*) are taken from the protein data bank.[32] The reaction center protein is from databank file 1L9B[33] and the cytochrome c_2 protein is from 1C2R.[34] We performed a series of mutations using *SYBYL*.[35] The single mutants for the reaction center protein are DK(L257), EK(M95), DK(M292), DK(L261), and DK(M184), and the single mutants for the cytochrome c_2 protein are KE(C99), KE(C93), KE(C54), KE(C32), and KE(C8) as in the experiments.[8] For these mutations, the charge changes by +2 e in the DK mutants, by −2 e in the KE mutants, and by +2 e in the EK mutants.

Diffusion Constants. The translational and rotational diffusion constants of the native reaction center and cytochrome c_2 were calculated using the Macrodox program.[14,15,36] The calculated translational and rotational diffusion constants are 0.449×10^{-2} Å^2/ps and 0.142×10^{-5} ps^{-1} for the native reaction center and 0.132×10^{-1} Å^2/ps and 0.364×10^{-4} ps^{-1} for the native cytochrome c_2, respectively. We assume that mutations will not change the translational and rotational diffusion constants.

Electrostatic Potential Calculations. Partial atomic charges were assigned to the proteins using the AMBER parameters in SDA.[37] At a neutral or near-neutral pH (in the experiments,[8] pH = 7.5), it is assumed that all lysines and arginines are protonated and the aspartic and glutamic acids and C-terminal groups are ionized.[38] The amino terminii are not protonated, and the histidines are singly protonated.[36] The partial atomic charges of the protein cofactors, including the heme, bacteriochlorophyll, bacteriochlorophyll dimer, bateriopheophytin, and ubiquinone, and the surfactants, including lauryl dimethylamine-*N*-oxide and heptane-1,2,3-triol were assigned from Mulliken charges calculated from the Gaussian program[39] using density functional theory with the B3LYP functional and 6-31G(d) basis set. First, the UHBD[40] program was used to calculate the electrostatic potentials of the proteins using the linearized finite-difference Poisson−Boltzmann equation. The dielectric constants were assigned to 4 inside the proteins and 78 outside. The solvent dielectric boundary was constructed by rolling a 1.5-Å radius probe on the van der Waals molecular surface of the proteins.[12] An ionic strength of 10 mM was used as in the experiments.[8] Grids of $150 \times 150 \times 150$ points^3 with a 1.0-Å spacing centered on each of the proteins were used to compute the electrostatic potentials. The effective charges[41,42] for each protein are defined as fitted charges that, when immersed in a uniform dielectric, give the electrostatic potential of the protein computed in a heterogeneous dielectric. The charges reproduce the electrostatic potential of a protein described with an all-atom description with an accuracy of 5−10% when only assigning effective charges to 1 or 2 atoms of the side chain of the titratable residues (these atoms are the carboxylate oxygen atoms of Asp, Glu, the C terminus, and the nitrogen atoms of Arg, Lys, and the N terminus). The effective charges were assigned using the ECM program of SDA.[37] (The effective

charges are fitted in SDA[37] with a procedure similar to the CHELP procedure.[43])

Electrostatic Desolvation Contributions. In SDA,[37] the desolvation energy of protein 1, due to the presence of protein 2, is approximated as[11]

$$\Delta G_{\text{desolvation}} \approx \alpha \frac{\epsilon_s - \epsilon_p}{\epsilon_s(2\epsilon_s + \epsilon_p)} \sum_{ij} (1 + \kappa r_{ij})^2 \times \exp(-2\kappa r_{ij}) \frac{q_i^2 a_j^3}{r_{ij}^4} \quad (8)$$

where ϵ_s is the solvent dielectric, ϵ_p is the protein dielectric, q_i is the effective charge on the ith atom of protein 1, a_j is the radius of the jth atom of protein 2, r_{ij} is the distance between the two atoms, and κ is the Debye−Hückel parameter[11]

$$\kappa = (8\pi N_A e^2/\epsilon k_B T)^{1/2} I^{1/2} \quad (9)$$

Here, N_A is Avogadro's number, I is the ionic strength, e is the electronic charge, k_B is Boltzmann's constant, T is temperature, and ϵ is the dielectric constant of the solvent. α is a scaling factor that is adjusted to optimize the agreement of the effective charges approximation with the full atomic electrostatics calculations by solving the linearized finite-difference Poisson−Boltzmann equation; $\alpha = 1.62$ was taken from ref 44.

The electrostatic interaction free energies were approximated using the sum of the effective charge interaction ($q_{\text{eff}}\phi$) terms and a charge desolvation term given by eq 8. Electrostatic forces and torques were calculated from the potential energies.

Brownian Dynamics Simulations. We modified the SDA[37] code by adding an exponential distance-dependent electron-transfer reaction criterion to the Brownian dynamics (BD) simulation,[16−18] and we computed the second-order electron-transfer rates for the native and mutant proteins. We chose 10 000 BD trajectories (see Results and Discussion section), an initial separation distance of $b = 500$ Å (where $r > b$, the interaction force is centrosymmetric), and a truncation surface distance of $c = 1000$ Å (large enough so that a significant fraction of trajectories is successful[30]). The experiments[7,8] show that the first-order electron-transfer rates do not change much among the mutants. We used a uniform $k_{et}^0 = 4.0 \times 10^{10}$ s^{-1} in eq 4 for all of the mutants (see Results and Discussion section). The decay factor in eq 4 is assigned to 0.9 Å^{-1}, [45] and d_0 in eq 4 is approximated as 12.64 Å, the minimum distance between the atoms of the π-electron porphyrin of cytochrome c_2 and the π-electron bacteriochlorophyll dimer of the reaction center in *Rhodobacter sphearoides* (the distance is estimated using the cocrystal structure of PDB file 1L9B[33]).

4. Results and Discussion

Sensitivity to the Number of Trajectories. To select a reasonable number of trajectories, we compared the computed second-order rates for trajectories ranging from 1000 to 200 000. When the number of trajectories increases from 1000 to 200 000 (Figure 1), the rate changes by about 30% and reaches saturation after 75 000. To save computation time, we used 10 000 trajectories, which we estimate will produce 30% error in our rates.

Determination of k_{et}^0 and β. In the model, k_{et}^0 and β are adjustable parameters.[16] We fitted the k_{et}^0 value in eq 4 for the native reaction center (RC) and cytochrome c_2 using Northrup's[18] approach. For a fixed decay factor $\beta = 0.9$ Å^{-1} in eq 4, we varied k_{et}^0. Figure 2 shows the dependence of the second-order electron-transfer rate constants on k_{et}^0. The bimolecular rates

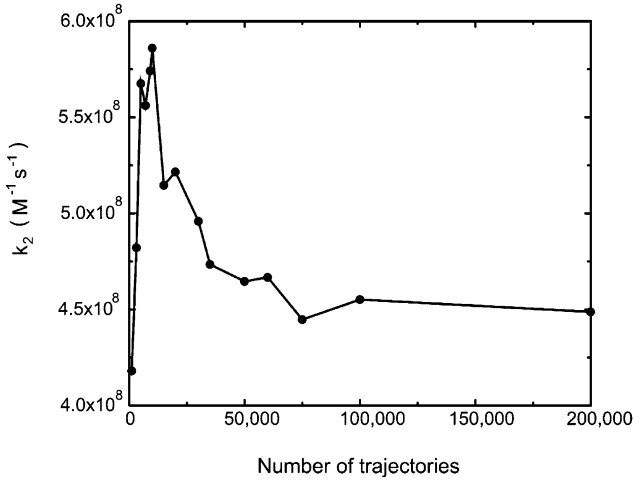

Figure 1. Sensitivity of the bimolecular rate to the number of trajectories.

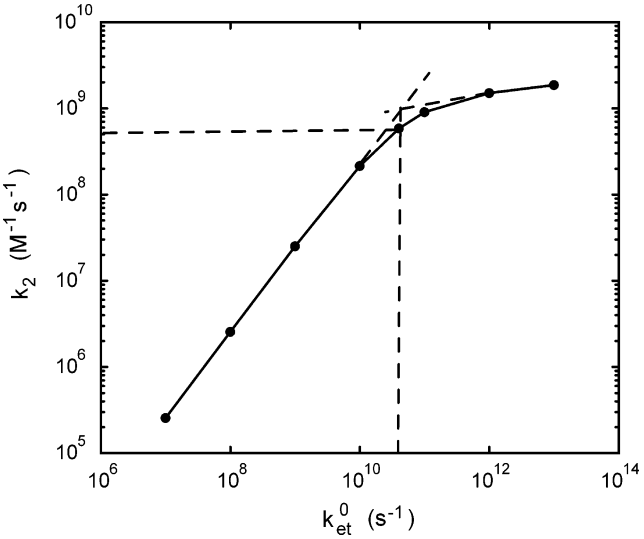

Figure 2. Dependence of the calculated bimolecular rate in the native proteins (k_2) on the choice of ET rate prefactor, k_{et}^0, for $\beta = 0.9$ Å^{-1}. In the remainder of the studies, we set $k_{et}^0 = 4.0 \times 10^{10}$ s^{-1} at which k_2 saturates for the native proteins and $k_2 = 0.6 \times 10^9$ M^{-1} s^{-1}, close to the experimental value of 1.6×10^9 M^{-1} s^{-1}.

increase nearly linearly with k_{et}^0 up to $k_{et}^0 = 4.0 \times 10^{10}$ s^{-1} and then saturate. The electron transfer for the native RC/cyt system is diffusion-limited.[46] So, the k_{et}^0 value we choose should be greater than or equal to $k_{et}^0 = 4.0 \times 10^{10}$ s^{-1}, which is the turning point from the activation-limited regime to the diffusion-limited regime. If we use Northrup's[18] approach to match the experimental second-order rate, 1.6×10^9 M^{-1} s^{-1},[8] k_{et}^0 will be larger than 10^{13} s^{-1}. The value of k_{et}^0 for a closest contact distance of 12.6 Å between the edges of the heme and the special pair redox species based on nonadiabatic ET rate theory with $\Delta G° = -0.5$ eV, $\lambda = 0.5$ eV (from ref 46), and $\beta = 0.9$ Å^{-1} is $5 \times 10^{10} \times H_0^2$ s^{-1}, where H_0^2 is the electronic coupling squared in units of eV^2 when the donor and acceptor are in direct contact. H_0^2 is expected to be 10^{-3} to 1 eV^2.[47,48] As such, k_{et}^0 based on nonadiabatic ET theory will be 5.0×10^7 s^{-1} to 5.0×10^{10} s^{-1}. Considering this range, we chose k_{et}^0 as 4.0×10^{10} s^{-1}, at which the k_{et}^0 value is plausible on the basis of nonadiabatic ET rate theory as well as leading to a diffusion-limited rate. The second-order rate computed using $k_{et}^0 = 4.0 \times 10^{10}$ s^{-1} is 0.6×10^9 M^{-1} s^{-1}, which is comparable to the experimental value of 1.6×10^9 M^{-1} s^{-1}.[8] The measured first-

TABLE 1: Comparison between Calculational (*c*) and Experimental (*E*) Second-Order ET Rate Constants ($\times 10^6$ M^{-1} s^{-1}) for Reaction Centers from *Rhodobactor sphaeroides* and Cyt c_2 from *Rhodobactor capsulatus* (including the double-mutant studies)

mutant	k_2^c	k_2^E	k_2^E/k_2^c	mutant	k_2^c	k_2^E	k_2^E/k_2^c
nat./nat.	586	1600	2.7	DK(L155)/KE(C54)	8.5	170	20
nat./KE(C8)	99	330	3.3	DK(L155)/KE(C93)	15	70	4.7
nat./KE(C32)	56	400	7.1	DK(L155)/KE(C99)	6.9	3.6	0.5
nat./KE(C54)	15	130	8.7	DK(M292)/nat.	74	700	9.5
nat./KE(C93)	52	79	1.5	DK(M292)/KE(C8)	24	170	7.1
nat./KE(C99)	17	23	1.4	DK(M292)/KE(C32)	25	80	3.2
DK(L257)/nat.	86	700	8.1	DK(M292)/KE(C54)	6.6	7.1	1.1
DK(L257)/KE(C8)	40	77	1.9	DK(M292)/KE(C93)	9.8	4.6	0.5
DK(L257)/KE(C32)	29	200	6.9	DK(M292)/KE(C99)	10	24	2.4
DK(L257)/KE(C54)	5.7	150	26	DK(L261)/nat.	46	300	6.5
DK(L257)/KE(C93)	4.6	50	11	DK(L261)/KE(C8)	25	13	0.5
DK(L257)/KE(C99)	8.0	2.9	0.4	DK(L261)/KE(C32)	8.8	57	6.5
EK(M95)/nat.	42	380	9.0	DK(L261)/KE(C54)	2.8	130	46
EK(M95)/KE(C8)	16	20	1.3	DK(L261)/KE(C93)	6.2	45	7.3
EK(M95)/KE(C32)	6.5	51	7.8	DK(L261)/KE(C99)	1.9	0.8	0.4
EK(M95)/KE(C54)	2.1	11	5.2	Dk(M184)/nat.	29	300	10
EK(M95)/KE(C93)	2.6	20	7.7	DK(M184)/KE(C8)	13	5.9	0.5
EK(M95)/KE(C99)	9.4	46	4.9	DK(M184)/KE(C32)	13	20	1.5
DK(L155)/nat.	70	730	10	DK(M184)/KE(C54)	1.0	11	11
DK(L155)/KE(C8)	33	87	2.6	DK(M184)/KE(C93)	6.4	18	2.8
DK(L155)/KE(C32)	18	300	17	DK(M184)/KE(C99)	4.8	57	12

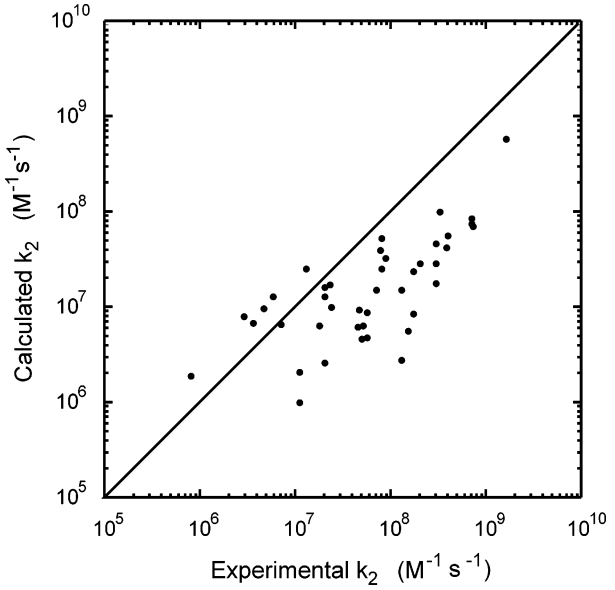

Figure 3. The correlation of calculated and experimental second-order rate constants (k_2) for the native RC/cyt c_2 and double mutants. $R = 0.872$.

order electron-transfer rate constant in the bound RC−cyt complex is 1.1×10^6 s^{-1}.[8] The measured value is an ensemble average. In the ensemble, the fraction of electron-transfer active conformations can be quite small,[20] so the rate constant associated with the ET active miniority conformations may be much larger than the observed first-order rate of 1.1×10^6 s^{-1}. The average β measured for proteins is 0.8−1.2 $Å^{-1}$.[49] For frozen water, β is measured to be 1.61−1.75 $Å^{-1}$.[49] The average β for a protein−water interface is expected to depend strongly on its structure.

Second-Order Rate Constants. Table 1 compares the calculated second-order rate constants for the native and mutant proteins with the experimental results from ref 8. Figure 3 shows the correlation between calculated and experimental rates.[8] The largest difference between the calculated and experimental rates for the mutants is a factor of 50, while most rates agree within a factor of 10. The rate for the native reaction center and native cytochrome c_2 pair is larger than the rate for any of the mutants. The theoretical results in Table 1 are also consistent with the range of mutant rates from 10^6 M^{-1} s^{-1} to 10^9 M^{-1} s^{-1}. The theoretical results semiquantitatively reproduce these experimental data.

TABLE 2: Second-Order Electron Transfer Rate Constants for Native Reaction Center/Cytochrome c_2 and DK(L261)/KE(C99) as a Function of Electron Transfer Pre-Exponential Factor k_{et}^0

k_{et}^0 (s^{-1})	k_2 (M^{-1} s^{-1}) (nat./nat.)	k_2 (M^{-1} s^{-1}) (DK(L261)/KE(C99))
4.0×10^{10}	5.86×10^8	1.93×10^6
1.0×10^{11}	9.04×10^8	4.75×10^6
1.0×10^{12}	1.51×10^9	3.80×10^7
1.0×10^{13}	1.86×10^9	1.45×10^8
1.0×10^{14}	2.20×10^9	3.56×10^8

Diffusion-Controlled and Activation-Controlled Rates. To probe the reaction mechanism, we varied k_{et}^0. For the diffusion-limited mechanism, the rate will not depend on this parameter. For the activation-limited mechanism, the rate will scale linearly with this parameter (see Appendix). Table 2 and Figure 4 show the second-order electron-transfer (ET) rate constants vary with k_{et}^0 for two systems: native RC/cytochrome c_2 and the DK(L261)/KE(C99) double mutant. For the native RC/cytochrome c_2 ET couple, the rate is predicted from this analysis to be diffusion-controlled, while for the DK(L261)/KE(C99) system, the rate is predicted to be activation-controlled. In the native system, the second-order rate holds approximately constant, while the value of k_{et}^0 in eq 4 is varied. In contrast, for the DK(L261)/KE(C99) system, the second-order rate increases approximately linearly with k_{et}^0 in eq 4 (it eventually saturates).

Ionic-Strength Dependence. Figure 5 shows the computed ionic-strength dependence of the second-order rate constant for the native RC/cytochrome c_2 system. The second-order rate constant decreases with increasing ionic strength, consistent with the screening of electrostatic interactions.[3,4,50] For myoglobin−cytochrome b_5 electron transfer, Hoffman and co-workers[20] found a similar ionic-strength dependence experimentally for the interprotein electron-transfer rate constant. There is a small dip in the curve in Figure 5 that may arise from undersampling.

5. Conclusions

For the first time, Brownian dynamics was used to analyze a particularly large electron-transfer system, the photosynthetic

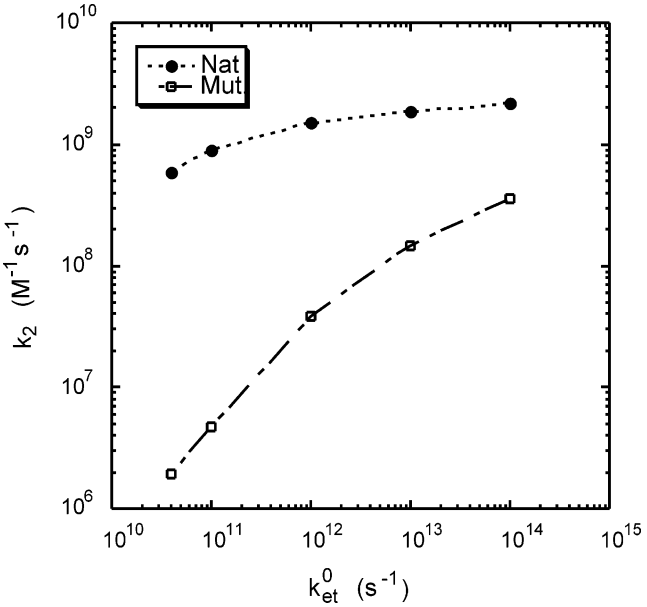

Figure 4. The second-order electron transfer rate constants for native reaction center/cytochrome c_2 and DK(L261)/KE(C99) as a function of electron transfer pre-exponential factor k^0_{et}.

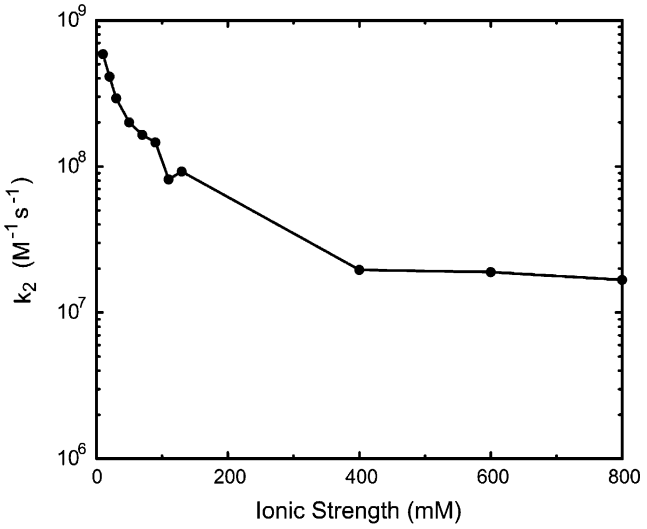

Figure 5. Theoretical ionic-strength dependence of the second-order rate constants (k_2) for native elactron transfer.

reaction center/cytochrome c_2 couple. The results are in agreement within an order of magnitude with the experimental data when reasonable prefactors and decay constants are employed. The analysis describes the influence of mutations on the reaction center/cytochrome c_2 system rates, which change by as much as 10^3. We predict that the second-order rate for the native reaction center/cytochrome c_2 system decreases with ionic strength. We found that mutations can switch the rate from the diffusion-limited to the activation-limited regime. These studies support the experimental conclusion regarding the role of electrostatic docking in the photosynthetic reaction center-cytochrome c_2 electron-transfer kinetics.[8]

Recently, a two-step mechanism for the protein−protein binding was presented:[24,51,52] The first step is diffusional association to form an encounter complex; the second step introduces rearrangement to form a more strongly bound ET active complex. Okamura and co-workers recently proposed adding a third state that represents further complex reorganization.[24] The Brownian dynamic simulations in this paper can describe the sequence of events in multistep models to the extent that the structures can be accessed within frozen protein surface models that are employed. The further development of models that would permit conformational changes of the proteins during encounters could provide a more complete theoretical description of the reaction dynamics. If protein surface rearrangement is essential for ET, the frozen geometry BD model used here will be incomplete. However, our simple model may describe some of the essential states that participate in ET. A judicious choice of ET parameters may approximately account for the omission of other key species.

In addition to the rigid-body assumption, we assumed an exponential distance-dependent electron-transfer model and a fixed ET rate prefactor. To improve the description of the electronic coupling, we could implement pathways[53−55] or more involved electronic structure analysis[56] of the electron tunneling interaction. A more detailed analysis of the desolvation energetics could further improve the calculations. Studies of the proteins in the geometry of the complex, or intermediate between the docked[33] and free structures, might also prove to be informative.

Acknowledgment. We thank NIH (GM-48043) for support of this research. We also thank Prof. M. Okamura, Prof. J. N. Onuchic, and Dr. M. Pasquinelli for helpful discussions.

Appendix

Rates for Bimolecular Reactions. In the steady-state approximation, the bimolecular reaction

$$A^* + B^+ \underset{k_{off}}{\overset{k_{on}}{\rightleftharpoons}} (A^*B^+) \xrightarrow{k_{et}} A^+ + B^*$$

is described by a second-order electron rate[57,58]

$$k_2 = k_{on} \times k_{et}/(k_{off} + k_{et}) \qquad (10)$$

The diffusion limit occurs when $k_{off} \ll k_{et}$ and $k_2 \approx k_{on}$. The activation limit occurs when $k_{off} \gg k_{et}$ and $k_2 \approx K_A \times k_{et}$ (where $K_A = k_{on}/k_{off}$).

References and Notes

(1) Feher, G.; Allen, J. P.; Okamura, M. Y.; Rees, D. C. *Nature (London)* **1989**, *339*, 111.
(2) Tiede, D.; Dutton, P. In *The Photosynthetic Reaction Center*; Deisenhofer, J.; Norris, J., Eds.; Academic Press: San Diego. 1993; p 258.
(3) Prince, R. C.; Cogdell, R. J.; Crofts, A. R. *Biochim. Biophys. Acta* **1974**, *347*, 1.
(4) Moser, C. C.; Dutton, P. L. *Biochemistry* **1988**, *27*, 2450.
(5) Venturoli, G.; Mallardi, A.; Mathis, P. *Biochemistry* **1993**, *32*, 13245.
(6) Tiede, D. M.; Vashista, A. C.; Gunner, M. R. *Biochemistry* **1993**, *32*, 4515.
(7) Tetreault, M.; Rongey, S. H.; Feher, G.; Okamura, M. Y. *Biochemistry* **2001**, *40*, 8452.
(8) Tetreault, M.; Cusanovich, M.; Meyer, T.; Axelrod, H.; Okamura, M. Y. *Bichemistry* **2002**, *41*, 5807.
(9) Wachtveitl, J.; Farchaus, J. W.; Mathis, P.; Oesterhelt, D. *Biochemistry* **1993**, *32*, 10894.
(10) Venturoli, G.; Drepper, F.; Williams, J. C.; Allen, J. P.; Lin, X.; Mathis, P. *Biophys. J.* **1998**, *74*, 3226.
(11) Elcock, A. H.; Gabdoulline, R. R.; Wade, R. C.; McCammon, J. A. *J. Mol. Biol.* **1999**, *291*, 149.
(12) Gabdoulline, R. R.; Wade, R. C. *J. Mol. Biol.* **2001**, *306*, 1139.
(13) De Rienzo, F. D.; Gabdoulline, R. R.; Menziani, M. C.; De Benedetti, P. G.; Wade, R. C. *Biophys. J.* **2001**, *81*, 3090.
(14) Northrup, S. H.; Reynolds, J. C. L.; Miller, C. M.; Forrest, K. J.; Boles, J. O. *J. Am. Chem. Soc.* **1986**, *108*, 8162.
(15) Northrup, S. H.; Boles, J. O.; Reynolds, J. C. L. *Science* **1988**, *241*, 67.
(16) Andrew, S. M.; Thomasson, K. A.; Northrup, S. H. *J. Am. Chem. Soc.* **1993**, *115*, 5516.

(17) Northrup, S. H.; Herbert, R. G. *Int. J. Quantum Chem.* **1990**, *17*, 55.
(18) Northrup, S. H.; Thomasson, K. A.; Miller, C. A. *Biochemistry* **1993**, *32*, 6613.
(19) Kidd, R. D.; Baker, E. N.; Brittain, T. *J. Biol. Inorg. Chem.* **2002**, *7*, 23.
(20) Liang, Z. X.; Kurnikov, I. V.; Nocek, J. M.; Mauk, A. G.; Beratan, D. N.; Hoffman, B. M. *J. Am. Chem. Soc.* **2003**, *126*, 2785.
(21) Aquino, A. J. A.; Beroza, P.; Reagan, J.; Onuchic, J. N. *Chem. Phys. Lett.* **1997**, *275*, 181.
(22) Aquino, A. J. A.; Beroza, P.; Beratan, D. N.; Onuchic, J. N. *Chem. Phys.* **1995**, *197*, 277.
(23) Miyashita, O.; Okamura, M. Y.; Onuchic, J. N. *J. Phys. Chem.* **2003**, *107*, 1230.
(24) Miyashita, O.; Onuchic, J. N.; Okamura, M. Y. *Biochemistry* **2003**, *42*, 11651.
(25) (a) Miyashita, O.; Onuchic, J. N.; Okamura, M. Y. *Proc. Natl. Acad. Sci. U.S.A.* **2004**, *101*, 16174. (b) Miyashita, O.; Okamura, M. Y.; Onuchic, J. N. *Proc. Natl. Acad. Sci. U.S.A.* **2005**, *102*, 3558.
(26) Autenrieth, F.; Tajkhorshid, E.; Schulten, K.; Luthey-Schulten, Z. *J. Phys. Chem. B* **2004**, *108*, 20376.
(27) Wlodek, S. T.; Shen, T.; McCammon, J. A. *Biopolymers* **2000**, *53*, 265.
(28) Wade, R. C.; Gabdoulline, R. R.; Lüdemann, S. K.; Lounnas, V. *Proc. Natl. Acad. Sci. U.S.A.* **1998**, *95*, 5942.
(29) Ermak, D. L.; McCammon, J. A. *J. Chem. Phys.* **1978**, *69*, 1352.
(30) Northrup, S. H.; Allison, S. A.; McCammon, J. A. *J. Chem. Phys.* **1984**, *80*, 1517.
(31) Smoluchowski, M. V. *Z. Phys. Chem.* **1917**, *92*, 129.
(32) Berman, H. M.; Westbrook, J.; Feng, Z.; Gilliland, G.; Weissig, H.; Shindyalov, I. N.; Bourne, P. E. *Nucleic Acids Res.* **2000**, *28*, 235.
(33) Axelrod, H. L.; Abresch, E. C.; Okamura, M. Y.; Yeh, A. P.; Rees, D. C.; Feher, G. *J. Mol. Biol.* **2002**, *319*, 501.
(34) Benning, M. M.; Wesenberg, G.; Caffrey, M. S.; Bartsch, R. G.; Meyer, T. E.; Cusanovich, M. A.; Rayment, I.; Holden, H. M. *J. Mol. Biol.* **1991**, *220*, 673.
(35) *SYBYL*, version 6.5 (MIPS3 − IRIX 6.2); Tripos, Inc.: St. Louis, MO, 1998.
(36) Northrup, S. H.; Boles, J. O.; Reynolds, J. C. L. *J. Phys. Chem.* **1987**, *91*, 5991.
(37) Gabdoulline, R. R.; Wade, R. C. *Methods* **1998**, *14*, 329.
(38) Matthew, J. B. *Annu. Rev. Biophys. Biophys. Chem.* **1985**, *14*, 387.
(39) Frisch, M. J.; Trucks, G. W.; Schlegel, H. B.; Scuseria, G. E.; Robb, M. A.; Cheeseman, J. R.; Zakrzewski, V. G.; Montgomery, J. A., Jr.; Stratmann, R. E.; Burant, J. C.; Dapprich, S.; Millam, J. M.; Daniels, A. D.; Kudin, K. N.; Strain, M. C.; Farkas, O.; Tomasi, J.; Barone, V.; Cossi, M.; Cammi, R.; Mennucci, B.; Pomelli, C.; Adamo, C.; Clifford, S.; Ochterski, J.; Petersson, G. A.; Ayala, P. Y.; Cui, Q.; Morokuma, K.; Malick, D. K.; Rabuck, A. D.; Raghavachari, K.; Foresman, J. B.; Cioslowski, J.; Ortiz, J. V.; Stefanov, B. B.; Liu, G.; Liashenko, A.; Piskorz, P.; Komaromi, I.; Gomperts, R.; Martin, R. L.; Fox, D. J.; Keith, T.; Al-Laham, M. A.; Peng, C. Y.; Nanayakkara, A.; Gonzalez, C.; Challacombe, M.; Gill, P. M. W.; Johnson, B. G.; Chen, W.; Wong, M. W.; Andres, J. L.; Head-Gordon, M.; Replogle, E. S.; Pople, J. A. *Gaussian 98*, revision A.11.3; Gaussian, Inc.: Pittsburgh, PA, 1998.
(40) Briggs, J. M.; Madura, J. D.; Davis, M. E.; Gilson, M. K.; Antosiewicz, J.; Luty, B. A.; Wade, R. C.; Bagheri, B.; Ilin, A.; Tan, R. C.; McCammon, J. A. *University of Houston Brownian Dynamics Program*; University of Houston: Houston, TX, 1989.
(41) Gabdoulline, R. R.; Wade, R. C. *J. Phys. Chem.* **1996**, *100*, 3868.
(42) http://www.embl-heidelberg.de/ gabdoull/ecm/index.html.
(43) Chirlain, L. E.; Francl, M. M. *J. Comput. Chem.* **1987**, *6*, 894.
(44) http://www.embl-heidelberg.de/ gabdoull/sda/sda.html# desolvg.
(45) Gray, H. B.; Malmström, B. G. *Biochemistry* **1989**, *28*, 7499.
(46) Lin, X.; Williams, J. C.; Allen, J. P.; Mathis, P. *Biochemistry* **1994**, *33*, 13517.
(47) Hopfield, J. J. *Proc. Natl. Acad. Sci. U.S.A.* **1974**, *15*, 155.
(48) Skourtis, S. S.; Beratan, D. N. *Adv. Chem. Phys.* **1999**, *106*, 377.
(49) Tezcan, F. A.; Crane, B. R.; Winkler, J. R.; Gray, H. B. *Proc. Natl. Acad. Sci. U.S.A.* **2001**, *98*, 5002.
(50) Ke, B.; Chaney, T. H.; Reed, D. W. *Biochim. Biophys. Acta* **1970**, *216*, 373.
(51) Gabdoulline, R. R.; Wade, R. C. *Curr. Opin. Struct. Biol.* **2002**, *12*, 204.
(52) Camacho, C. J.; Vajda, S. *Curr. Opin. Struct. Biol.* **2002**, *12*, 36.
(53) Beratan, D. N.; Betts, J. N.; Onuchic, J. N. *Science* **1991**, *252*, 1285.
(54) Beratan, D. N.; Onuchic, J. N.; Hopfield, J. J. *J. Chem. Phys.* **1987**, *86*, 4488.
(55) Onuchic, J. N.; Beratan, D. N. *J. Chem. Phys.* **1990**, *92*, 722.
(56) Kurnikov, I. V.; Beratan, D. N. *J. Chem. Phys.* **1996**, *105*, 9561.
(57) Bendall, D. S. In *Protein Electron Transfer*;Bendall, D. S., Ed.; Bios Scientific Publishers: Cambridge, U.K., 1996; p 43.
(58) Davidson, V. L. *Acc. Chem. Res.* **2000**, *33*, 87.